

# Worst-case and Distributional Robustness Analysis of a Thin Film Deposition Process

Shabnam Rasoulia, Luis A. Ricardez-Sandoval

*Department of Chemical Engineering, University of Waterloo, N2L 3G1, Waterloo, Canada  
(Tel: +1 519 888 4567 ext.38667; e-mail: s4rasoul@uwaterloo.ca, laricard@uwaterloo.ca).*

---

**Abstract:** This paper presents a comparison between worst-case and distributional uncertainty analysis in a thin film deposition process. The key idea is to evaluate the effect of model parameter uncertainties on thin film properties employing power series expansion (PSE). The worst-case deviation in the film properties is obtained under bounded parameter uncertainties while the probabilistic bounds are estimated under distributional uncertainties. To describe the growth process on the surface of a substrate, a multiscale approach that integrates kinetic Monte Carlo (KMC) simulations with continuum modelling is employed. The uncertainty analysis in this work is applied to estimate the optimal substrate temperature profile for robust optimization of the thin film end-point properties.

**Keywords:** Thin film deposition, Multiscale modelling, Uncertainty analysis, Power series expansion, Robust optimization.

---

## 1. INTRODUCTION

Thin film deposition is a critical step in semiconductor manufacturing that has motivated significant research efforts towards process modelling, optimization and control to produce efficient electronic devices at low cost. Despite the extensive body of research, there are still many unresolved issues leading to a significant gap between the expected and the actual performance achieved by the current control methodologies (Christofides & Armaou, 2006). This gap is mainly related to the complexities associated with the multiscale nature of the thin film deposition process, lack of practical and reliable online *in-situ* sensors at the micro-scale level, and uncertainties in the mechanisms and parameters of the system (Vlachos, 2005; Ricardez-Sandoval, 2011). The disparity in length and time scales of the physicochemical events occurring in thin film deposition is often described using a continuum deterministic model coupled with discrete stochastic kinetic Monte Carlo (KMC) simulations describing the evolution of the thin film at the surface (Lam & Vlachos, 2001). Unlike continuum models, the KMC approach does not provide a closed-form model needed for model-based control and optimization and is also computationally prohibitive for online applications. Approaches based on lattice-based KMC simulations or model reductions have been employed to estimate the film's microstructure (Gallivan & Murray, 2004; Lou & Christofides, 2003).

Although the recently introduced optical *in-situ* sensors have triggered research on feedback control of the thin film deposition process, their application is still limited in practice. In industry, most of the measurements are available at the end of the process; accordingly, optimization and control approaches that do not have access to online fine-scale measurements need to be developed. The deposition

process is a batch process where open-loop process optimization can be performed offline, based on certain product quality requirements. It has been shown that an optimal change in the precursor concentration reduces considerably the thickness non-uniformity in a GaN thin film (Varshney & Armaou, 2006). One key challenge in the implementation of model-based approaches is model-process mismatch. The lack of knowledge about the mechanisms and parameters at the fine-scale has motivated experimental design studies for parameter optimization (Prasad & Vlachos, 2008). Another way to address uncertainties is to design robust frameworks that prevent the loss in the optimization or control objectives. The uncertainty effects are quantified in the desired outputs and an objective function is defined such that it produces a robust performance. In model-based control of semiconductor processes, power series expansion (PSE) has been applied for robust optimization of end-point properties in thin films and junctions required in microelectronic devices (Gunawan, et al., 2004; Nagy & Allgower, 2007; Rasoulia & Ricardez-Sandoval, 2014). In a recent work, PSEs have been applied to identify closed-form models that predict the outputs of the process for a nonlinear model predictive control approach under uncertainty (Rasoulia & Ricardez-Sandoval, 2015).

A fundamental step in robust optimization, however, is the characterization of uncertainty in model parameters. Due to difficulties in determining the type of uncertainties, the common assumption is that the uncertainties are either normally distributed or bounded. The probabilistic approach based on normal distribution leads to optimistic estimates whereas the worst-case scenario via bounded uncertainties might include realizations in the parameters that will be very unlikely thus leading to overly conservative results. In this

work, these two approaches are compared on a thin film deposition process based on the PSEs. Although the methods employed in this work are well-known uncertainty analysis approaches for robust optimization, their implementation for the present multi-scale thin film deposition model has not been studied before. The required sensitivities in the expansions are obtained by central finite differences using average of multiple multiscale simulations describing the deposition process. To show the effectiveness of this approach, the uncertainty analysis has been embedded within an optimization framework to seek for the robust optimal substrate temperature profile that maximizes the end-point thickness of the film under surface roughness and growth rate constraints.

## 2. THIN FILM DEPOSITION PROCESS

In this work, an epitaxial thin film deposition process on a substrate from gas precursors in a reactor chamber is considered. In this process, gas enters perpendicular to the substrate and forms a boundary layer adjacent to the surface. The gas atoms diffuse the boundary layer and through microscopic phenomena form a solid thin film on the substrate. The multiscale nature of the process is modelled using macro-scale continuum partial differential equations (PDEs) embedded with micro-scale KMC simulations (Lam & Vlachos, 2001).

### 2.1. Gas phase model

At the macroscopic level, continuum descriptions of fluid flow, heat transfer and mass transfer can be employed (Song, et al., 1991):

$$\frac{\partial}{\partial \tau} \left( \frac{\partial f}{\partial \eta} \right) = \frac{\partial^3 f}{\partial \eta^3} + f \frac{\partial^2 f}{\partial \eta^2} + \frac{1}{2} \left[ \frac{\rho_b}{\rho} - \left( \frac{\partial f}{\partial \eta} \right)^2 \right], \quad (1)$$

$$\frac{\partial T}{\partial \tau} = \frac{1}{Pr} \frac{\partial^2 T}{\partial \eta^2} + f \frac{\partial T}{\partial \eta}, \quad (2)$$

$$\frac{\partial x}{\partial \tau} = \frac{1}{Sc} \frac{\partial^2 x}{\partial \eta^2} + f \frac{\partial x}{\partial \eta}. \quad (3)$$

The boundary conditions for the bulk ( $\eta \rightarrow \infty$ ) are:

$$\frac{\partial f}{\partial \eta} = 1, T = T_{bulk}, x = x_b. \quad (4)$$

Likewise, the boundary conditions on the surface ( $\eta \rightarrow 0$ ) are:

$$f = 0, \frac{\partial f}{\partial \eta} = 0, T = T_{surface}, \quad (5)$$

$$\frac{\partial x}{\partial \eta} = \frac{Sc(R_a - R_d)}{\sqrt{2a\mu_b\rho_b}}. \quad (6)$$

In (1)-(6),  $f$  denotes the dimensionless stream function,  $\eta$  is the dimensionless distance to the surface,  $\rho$  is the density of the mixture,  $Pr$  is the Prandtl number,  $x$  and  $Sc$  are the mole fraction and Schmidt number of species, respectively. The parameters,  $\mu_b$ ,  $\rho_b$  and  $x_b$ , are the viscosity, density and the precursor's mole fraction of the bulk, respectively;  $a$  is the hydrodynamic strain rate and  $\tau = 2at$  is the dimensionless time.  $R_a$  and  $R_d$  correspond to the rates of adsorption and desorption, respectively.

### 2.2. Thin film surface model

The microscopic events considered in the current model include adsorption, desorption and migration of the atoms on

the surface of the thin film. To reduce the computational costs, the method has been implemented for a limited-size lattice with periodic boundary conditions. Moreover, the deposition follows the solid-on-solid approximation and only first nearest neighbours interactions are considered between the adsorbed atoms. The total adsorption rate is assumed to be site-independent and is calculated from the kinetic theory of the ideal gases as follows:

$$W_a = \frac{S_0 P x_{grow} N^2}{\sqrt{2\pi m R T} C_{tot}}, \quad (7)$$

where  $S_0$  is the sticking coefficient,  $P$  is the total pressure of gas phase,  $x_{grow}$  is the mole fraction of precursor on the surface,  $C_{tot}$  is the concentration of sites on the surface,  $m$  is the precursor molecular weight,  $N$  is the lattice size in KMC simulations,  $R$  is the gas constant and  $T$  is the substrate temperature.

Total rates of desorption and migration on the surface follow Arrhenius kinetics and depend on the local configuration of the surface. The total rate of desorption is calculated by:

$$W_d = \sum_{i=1}^5 k_{d0} M_i \exp(-(iE + E_d)/RT), \quad (8)$$

where  $M_i$  is the number of surface atoms with  $i$  nearest neighbours.  $E$  is the energy associated with a single bond on the surface,  $E_d$  is the energy associated with desorption and  $k_{d0}$  is an event-frequency constant. Likewise, the total rate of migration is estimated as follows:

$$W_m = \sum_{i=1}^5 k_{d0} M_i \exp(-(iE + E_m)/RT), \quad (9)$$

where  $E_m$  is the energy associated with migration. At every step in the KMC simulations, the rates are calculated and an event (i.e., adsorption, desorption or migration) is selected and executed randomly by using a uniform random number. Once the event is executed, the time increment is calculated:

$$dt = -\frac{\ln \zeta}{W_a + W_d + W_m}, \quad (10)$$

where  $\zeta$  is a uniform random number from a (0,1) interval and  $dt$  is the time increment in the KMC model.

The continuum and the KMC models are linked at the solid-gas interface in order to couple the events occurring at different time scales in this process. To account for the effect of the transport phenomena in the gas phase on the growth process, the parameter of the adsorption rate at the microscopic scale, i.e.  $x_{grow}$ , is provided from the mass transfer balance shown in (3). The microscopic events on the surface, on the other hand, determine the boundary condition of the mass transfer equation, i.e. the adsorption and desorption events influence the net flux of the precursor on the surface.  $R_a$  and  $R_d$  in (6), respectively correspond to adsorption and desorption events; the difference between these values can be obtained as follows:

$$R_a - R_d = \frac{N_a - N_d}{2a N^2 \Delta T}, \quad (11)$$

where  $\Delta T$  is the coupling time instance between the macroscopic and the microscopic simulations.  $N_a$  is the number of adsorbed atoms during  $\Delta T$  and  $N_d$  is the number of

desorbed atoms in the same time interval. Parameters of the process studied in this work are shown in Table 1.

Table 1. Model parameters

Parameter	Value
$a$	5 1/s
$C_{tot}$	$1.6611 \times 10^{-5}$ sites.mol/m <sup>2</sup>
$E$	17000 cal/mol
$E_d$	17000 cal/mol
$E_m$	10200 cal/mol
$k_{d0}$	$1 \times 10^9$ 1/s
$m$	0.028 kg/mol
$P$	$1 \times 10^5$ Pa
$S_0$	0.1
Sc	0.75
$x_b$	$2 \times 10^{-6}$
$\mu_b \rho_b$	$9 \times 10^{11}$
$\rho_b / \rho$	1

The quality of the thin film microstructure is mostly determined by the surface roughness that can be estimated based on the average of the broken bonds on the surface (Rasoulia & Ricardez-Sandoval, 2014):

$$r = 1 + \frac{\sum(|h_{i+1,j}-h_{i,j}|+|h_{i-1,j}-h_{i,j}|+|h_{i,j+1}-h_{i,j}|+|h_{i,j-1}-h_{i,j}|)}{2N^2}, \quad (12)$$

where  $h_{i,j}$  is the surface height or number of atoms at site  $(i,j)$ . Growth rate and film thickness are another important control objectives in order to prevent an undergrown film at the end of the batch process. Thickness can be represented by the average height on the surface as follows:

$$H = \frac{1}{N^2} \sum_{i,j} h_{i,j}. \quad (13)$$

Growth rate is determined using the difference of adsorbed and desorbed atoms:

$$Gr = \frac{\sum_{i,j} \Delta h_{i,j}}{N^2 \Delta t}, \quad (14)$$

where  $\Delta h_{i,j} = h_{i,j}(t + \Delta t) - h_{i,j}(t)$  is the change in the surface height at site  $(i,j)$  during  $\Delta t$ .  $\Delta t$  is a specific time interval where the growth rate needs to be estimated.

From the modelling point of view, the evolution of the thin film encompasses microscopic processes that are subject to model parameter uncertainty. As shown in Table 1, the KMC model includes parameters that have to be either measured or inferred through fine-scale experimental data. The estimation of these parameters is not trivial and most of the values are not known with absolute certainty due to the limited and noisy measurements. The performance of model-based control and optimization approaches, on the other hand, is

affected by the accuracy of the model, and uncertainties can lead to significant losses in performance. To quantify the influence of uncertainties, the deviations in system's performance can be evaluated by performing an uncertainty analysis.

### 3. WORST-CASE AND PROBABILISTIC BOUNDS USING PSE

For uncertainty analysis, the perturbed model parameter vector,  $\theta \in \mathbb{R}^{n_\theta}$  is as follows:

$$\theta = \hat{\theta} + \delta\theta, \quad (15)$$

where  $\hat{\theta}$  is the nominal model parameter vector and  $\delta\theta$  is the perturbation about  $\hat{\theta}$ . The objective is to analyse the deviation in the system's output from the nominal output, i.e.,

$$\delta y = y - \hat{y}, \quad (16)$$

where  $\hat{y}$  is the output when the system is operated with the nominal model parameter  $\hat{\theta}$  and  $y$  is the output when parameter vector  $\theta$  is used. Analytical mathematical tools have been proposed to quantify the impact of parameter uncertainties on the system's performance (Nagy & Braatz, 2003). In this study, the deviation from the nominal output,  $\delta y$ , is computed using PSEs as follows:

$$\delta y = \mathbf{J}(t)\delta\theta + \delta\theta^T \mathbf{H}(t)\delta\theta + \dots, \quad (17)$$

where  $\mathbf{J}(t) = (dy(t)/d\theta)_{\hat{\theta}} \in \mathbb{R}^{n_\theta}$  and  $\mathbf{H}(t) = (d^2y(t)/d\theta^2)_{\hat{\theta}} \in \mathbb{R}^{n_\theta \times n_\theta}$  are respectively the Jacobian and Hessian evaluated around  $\hat{\theta}$  at a specific time,  $t$ .

Although the order of the series expansion depends on the process nonlinearity and variability in the uncertain parameters, first or second-order expansions are usually sufficient for engineering applications.

#### 3.1. Worst-case performance under bounded uncertainties

In the worst-case robustness analysis, the worst-case deviation in the system's output is evaluated under bounded uncertainties in the model parameters, i.e.,

$$\theta = \{\theta_l | \theta_l \leq \theta \leq \theta_u\}, \quad (18)$$

where  $\theta_l$  and  $\theta_u$  represent the lower and upper limits. The effect of this parameter uncertainty on the system's output can be estimated from the following optimization problem:

$$\max_{\theta_l \leq \theta \leq \theta_u} |\delta y| \quad (19)$$

Using first-order PSE, the worst-case variability in a process output,  $\delta y$ , is calculated as follows:

$$\delta y_{w.c} = \max_{\theta_l \leq \theta \leq \theta_u} |\mathbf{J}\delta\theta|. \quad (20)$$

More accurate estimates of the worst-case variability can be obtained by adding more terms into the expansion and can be formulated in terms of the skewed structured singular value (SSV) or  $\mu$  analysis (Braatz, et al., 1994). For the second-order PSE,  $\delta y_{w.c}$  can be obtained as follows:

$$\delta y_{w.c} = \max_{\theta_l \leq \theta \leq \theta_u} |\mathbf{J}\delta\theta + \delta\theta^T \mathbf{H}\delta\theta| \stackrel{\Leftrightarrow}{=} \max_{\mu_\Delta(\mathbf{M}) \geq \gamma} \gamma, \quad (21)$$

where

$$\mathbf{M} = \begin{bmatrix} \mathbf{0} & \mathbf{0} & \gamma\boldsymbol{\omega} \\ \gamma\mathbf{H} & \mathbf{0} & \gamma\mathbf{H}\mathbf{z} \\ \mathbf{z}^T\mathbf{H} + \mathbf{J} & \mathbf{W}_0^T & \mathbf{z}^T\mathbf{H}\mathbf{z} + \mathbf{J}\mathbf{z} \end{bmatrix}. \quad (22)$$

The  $\mathbf{0}$  in  $\mathbf{M}$  denotes a zero matrix of consistent dimensions;  $\boldsymbol{\omega} = 0.5(\boldsymbol{\theta}_u - \boldsymbol{\theta}_l)$  and  $\mathbf{z} = 0.5(\boldsymbol{\theta}_u + \boldsymbol{\theta}_l)$ .  $\Delta = \text{diag}(\Delta_r, \Delta_r, \delta_c)$  is the perturbation block in the  $\mu$  analysis.  $\delta_c$  is a complex scalar while  $\Delta_r$  consists of real scalars.

### 3.2. Probabilistic bounds under distributional uncertainty

In probabilistic-based approaches, the uncertainties in the parameters are mostly described by a multivariate normal distribution around the nominal parameter estimates as follows:

$$\varepsilon_\theta = \{\boldsymbol{\theta} | \delta\boldsymbol{\theta}^T \mathbf{V}_\theta^{-1} \delta\boldsymbol{\theta} \leq \chi_{n_\theta}^2(\alpha)\}, \quad (23)$$

where  $\mathbf{V}_\theta \in \mathbb{R}^{n_\theta \times n_\theta}$  denotes the positive definite covariance matrix,  $\chi_{n_\theta}^2$  is a chi-squared distribution with  $n_\theta$  degrees of freedom and  $\alpha$  is the confidence level. Assuming that the process can be accurately described using a first-order PSE, the normal distribution of the output can be obtained from:

$$f(y) = \frac{1}{\sqrt{2\pi|\mathbf{V}_\theta|}} \exp\left(-\frac{(y-\hat{y})^2}{2|\mathbf{V}_\theta|}\right) \quad (24)$$

For second and higher order PSEs, however, the distribution cannot be estimated analytically. Thus, random Monte Carlo realizations from the distributions of the parameters are needed to propagate the uncertainty. Once the output distribution is obtained either analytically or via the Monte Carlo sampling method, the probabilistic upper and lower bounds can be estimated at a specific probability:

$$y^b = F^{-1}(\mathbb{P}|y) = \{y: F(y)\}, \quad (25)$$

where  $b \in \{low, up\}$  and  $F^{-1}(\mathbb{P}|y)$  represents the inverse of cumulative distribution function evaluated at a predefined probability,  $\mathbb{P}$ .

## 4. ROBUST END-POINT OPTIMIZATION OF THIN FILM PROCESS

Microelectronic market imposes stringent requirements upon thin film properties including specific thickness and surface roughness. While the thickness of the thin film needs to be maximized for a finite batch time, the surface roughness has to be minimized to assemble high-performance electronic devices. These are two conflicting objectives since thick films can be obtained at low temperatures whereas smooth film surfaces can only be realized at relatively high temperatures. In addition, uncertainties lead to product quality variability resulting in a potential loss in profits. Thus, a key objective is to optimize the process performance under uncertainty. In most thin film control and optimization studies, the desired thin film is achieved by imposing an optimal substrate temperature profile during the deposition process. In this approach, the batch time,  $t_f$  is divided into  $K$  equally spaced time intervals while the temperature at each time interval,  $T(k)$  is kept piecewise constant between successive intervals and is considered as one of the decision variables in the optimization problem. Thus, the optimal control formulation considered in this study is as follows:

$$\max_{T(k)} H^{low}(t_f)$$

Subject to:

Multiscale model, (1)-(11)

$$h_1(k) = T_{min} - T(k) \leq 0$$

$$h_2(k) = T(k) - T_{max} \leq 0$$

$$h_3 = r^{up}(t_f) - r_{max} \leq 0 \quad (26)$$

$$h_4 = Gr_{min} - Gr^{low}(t_f) \leq 0$$

$$h_5 = dr^{up}(t_f)/dt - \epsilon \leq 0$$

$$h_6 = dGr^{low}(t_f)/dt - \epsilon \leq 0$$

$$t = [0, t_f]; \forall k = 1, 2, \dots, K$$

where the constraints  $h_1$  and  $h_2$  ensure that the temperature profile remains within the feasible operating region for the deposition process. Constraints  $h_3$  and  $h_4$  specify the maximum allowed surface roughness,  $r_{max}$  to satisfy market demands and the minimum growth rate,  $Gr_{min}$  to ensure process productivity, respectively. Moreover,  $h_5$  and  $h_6$  ensure minimum variability of these properties at the end of the batch. The superscripts *low* and *up* correspond to the end-point properties evaluated via the lower and upper bounds, respectively. As mentioned in the previous section, the bounds can be obtained by either probabilistic or worst-case scenario approaches.

In our previous work, an algorithm was proposed to propagate the time-varying uncertainties into rates of microscopic events and then the probabilistic bounds on the outputs were computed through KMC simulations (Rasoulia & Ricardez-Sandoval, 2014). In this work, however, these parameters are assumed to be constant unknown values during the batch but they can change randomly from batch to batch. Thus, uncertainties are propagated directly into system's outputs using PSEs. Therefore, although the formulation shown in (26) is similar to that used in our previous work, the algorithm employed here to solve this optimization problem is different as described above.

The uncertainties in the process are assumed in the energy associated with a single bond, and the bulk precursor mole fraction, i.e.  $\boldsymbol{\theta}^T = [E, x_b]$ . Problem (26) was solved under the assumption of bounded parametric uncertainty and distributional uncertainty in  $E$  and  $x_b$ , respectively. In the case of parametric uncertainty, the parameters  $E$  and  $x_b$  are described as follows:

$$E = \hat{E}(1 + \omega_E), x_b = \hat{x}_b(1 + \omega_{x_b}), \quad (27)$$

where the nominal values ( $\hat{E}$  and  $\hat{x}_b$ ) are given in Table 1 and the uncertainties are:

$$-0.2 \leq \omega_E \leq 0.2, -0.2 \leq \omega_{x_b} \leq 0.2 \quad (28)$$

For a fair comparison between the worst-case scenario and probabilistic bounds, the covariance matrix in distributional uncertainty is constructed such that 99.7% of the uncertain parameters are within the bounded uncertainties (three standard deviations rule); therefore,

$$\mathbf{V}_\theta = \begin{pmatrix} (0.2\hat{E}/3)^2 & 0 \\ 0 & (0.2\hat{x}_b/3)^2 \end{pmatrix} \quad (29)$$

A second-order PSE was employed to describe the effect of uncertainties on the surface roughness whereas first-order PSEs were sufficient to propagate uncertainties in thickness and growth rate. The sensitivities in the expansions were calculated using finite differences from the average of the outputs obtained through multiple multiscale models employing reduced-order lattices in the KMC simulations. To estimate upper and lower bounds, three different approaches were considered while solving optimization problem defined in (26): *i*) worst-case deviation in the outputs using description (27), *ii*) probabilistic bounds on outputs at 99.7% confidence interval, i.e.  $\mathbb{P} = 3\sigma$  in (25), and *iii*) probabilistic bounds at 68% confidence interval ( $\mathbb{P} = \sigma$  in (25)) using description (29). In the case of the worst-case scenario, the roughness at the end of the batch is estimated using SSV analysis as shown in Section 3.1 while the worst-case deviations in thickness and growth rate can be calculated analytically since they are described using first-order PSEs. On the other hand, to propagate the uncertainty in surface roughness in the probabilistic-based approaches, Monte Carlo sampling is applied to the second-order PSE as explained in Section 3.2 whereas the bounds on thickness and growth rate are obtained analytically using first-order PSEs.

The batch time was divided into ten equally spaced time intervals. For better comparison of the results, the initial temperature was fixed at 800 K. Fig. 1 presents the optimal temperature profiles obtained from (26) using the three approaches considered in this work. These profiles correspond to specifications in  $r_{max}$  and  $Gr_{min}$  of 7 mL and 13 mL/s, respectively.  $T_{min}$  and  $T_{max}$  were set to 600 and 1200 K, respectively. As shown in this figure, the optimal temperature profile demands low temperatures at earlier stages of the deposition process to maximize the thickness by high adsorption rates. However, close to end of the batch process, high substrate temperatures are needed to promote migration on the surface and meet the constraints on surface roughness. The profile obtained using 99.7% confidence interval in probabilistic approach is slightly different from the profile obtained using the worst-case scenario approach. However, the temperature profile based on 68% confidence interval is the most optimistic, since this approach estimates less conservative bounds on surface roughness. Note that other reasonable product specification constraints result in similar conclusions to that presented here.

Fig. 2 shows the bounds evaluated for surface roughness using the optimal temperature profiles shown in Fig. 1. As depicted in this figure, the bounds obtained by the worst-case scenario approach using the SSV analysis are more conservative compared to the bounds obtained using the probabilistic-based approach. The worst-case bounds are computed using the worst-case deviation from the nominal outputs. Moreover, this figure also shows 100 random open-loop variations of the surface roughness under bounded uncertainty (27) using the temperature profile obtained from the worst-case scenario. As shown in this figure, the roughness during the batch is bounded within upper and

lower bounds estimated based on the worst-case deviation whereas they violate the probabilistic-based bounds. The final film thicknesses employing these temperature profiles are given in Table 2. As expected, the worst-case scenario approach returned the most conservative film thickness at the end of the batch.

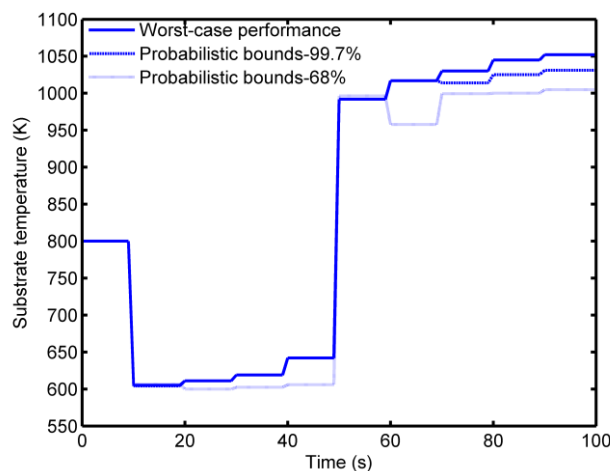


Fig. 1. Robust optimal temperature profiles using different approaches

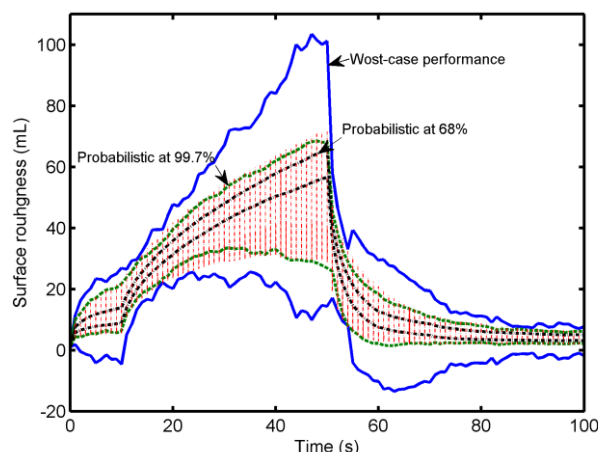


Fig. 2. Upper and lower bounds on surface roughness using different approaches and open-loop simulations using the temperature profile obtained for worst-case performance

Fig. 3 shows the final properties obtained under bounded parametric uncertainty using the temperature profiles obtained from these three approaches. As shown in this figure, regardless of a few violations using the temperature profile estimated by the probabilistic approach with 68% confidence interval, the three estimated optimal temperature profiles satisfy the constraints imposed on the optimization problem (26). That is, the final roughness of the thin film is mostly less than 7 mL in reality, even if the most optimistic temperature profile estimated by the probabilistic approach with 68% confidence interval is being used. In essence, the measurable benefits in using the worst-case scenario will be limited since it results in an overly conservative temperature profile that may eventually lead to economic losses. In

practice, the probabilistic approach with 68% confidence interval not only achieves an acceptable roughness, but also results in larger thickness and larger growth rate. This is a direct consequence of the optimistic temperature profile identified from the present approach.

Table 2. Optimal end-point thickness

Approach	Thickness (1000 mL)
Worst-case scenario	1.4595
Probabilistic at 99.7%	1.4759
Probabilistic at 68.0%	1.7293

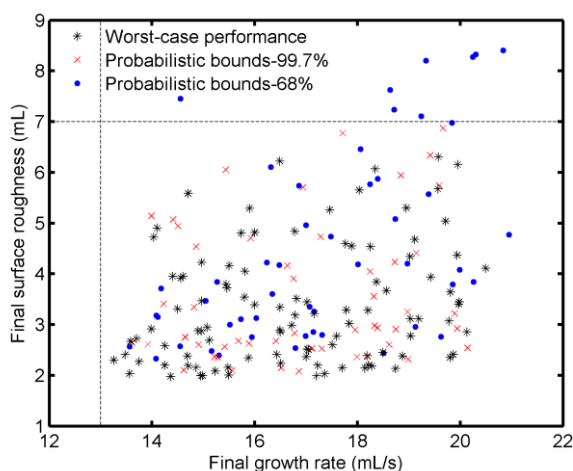


Fig. 3. Variation of final properties due to bounded parameter uncertainties, obtained from open-loop simulations applying various temperature profiles.

## 5. CONCLUSIONS

The aim of this paper is to compare the uncertainty analysis of the thin film deposition applying worst-case and probabilistic-based approaches. The sensitivities are obtained from average of multiple multiscale simulations employing reduced-order lattices in the KMC simulations. The optimal temperature profile that maximizes the final thickness of the thin film under end-point product constraints and uncertainty in the model parameters was identified. The results show that the prior assumption on type of the uncertainty affects the optimization results. Thus, inaccurate uncertainty description assumptions can lead to a loss in performance and therefore economic losses in the process.

## REFERENCES

Braatz, R. P., Young, P. M., Doyle, J. C. & Morari, M., 1994. Computational complexity of mu calculation. *IEEE Transaction on Automatic Control*, Volume 39, pp. 1000-1002.

Christofides, P. D. & Armaou, A., 2006. Control and optimization of multiscale process systems. *Computers & Chemical Engineering*, Volume 30, pp. 1670-1686.

Gallivan, M. A. & Murray, R. M., 2004. Reduction and identification methods for Markovian control systems, with

application to thin film deposition. *International Journal of Robust and Nonlinear Control*, Volume 14, pp. 113-132.

Gunawan, R., Jung, M. Y. L., Seebauer, E. G. & Braatz, R. D., 2004. Optimal control of rapid thermal annealing in a semiconductor process. *Journal of Process Control*, Volume 14, pp. 423-430.

Lam, R. & Vlachos, D. G., 2001. Multiscale model for epitaxial growth of films: Growth mode transition. *Physical Review B*, Volume 64, p. 035401.

Lou, Y. & Christofides, P. D., 2003. Estimation and control of surface roughness in thin film growth using kinetic Monte-Carlo models. *Chemical Engineering Science*, Volume 58, pp. 3115-3129.

Nagy, Z. K. & Allgower, F., 2007. A nonlinear model predictive control approach for robust end-point property control of a thin-film deposition process. *International Journal of Robust and Nonlinear Control*, Volume 17, pp. 1600-1613.

Nagy, Z. K. & Braatz, R. D., 2003. Worst-case and distributional robustness analysis of finite-time control trajectories for nonlinear distributed parameter systems. *IEEE Transactions on Control Systems Technology*, Volume 11, pp. 694-704.

Prasad, V. & Vlachos, D. G., 2008. Multiscale model and informatics-based optimal design of experiments: Application to the catalytic decomposition of ammonia on ruthenium. *Industrial & Engineering Chemistry*, Volume 47, pp. 6555-6567.

Rasoulilian, S. & Ricardez-Sandoval, L., 2015. A robust nonlinear model predictive controller for a multiscale thin film deposition process. *Chemical Engineering Science*, <http://dx.doi.org/10.1016/j.ces.2015.02.002i>.

Rasoulilian, S. & Ricardez-Sandoval, L. A., 2014. Uncertainty analysis and robust optimization of multiscale process systems with application to epitaxial thin film growth. *Chemical Engineering Science*, Volume 116, pp. 590-600.

Ricardez-Sandoval, L. A., 2011. Current challenges in the design and control of multiscale systems. *The Canadian Journal of Chemical Engineering*, Volume 89, pp. 1324-1341.

Song, X., Williams, W. R., Schmidt, L. D. & Aris, R., 1991. Bifurcation behavior in homogeneous-heterogeneous combustion: II. computations for stagnation point flow. *Combustion and Flame*, Volume 84, pp. 292-311.

Varshney, A. & Armaou, A., 2006. Optimal operation of GaN thin film epitaxy employing control vector parameterization. *AIChE Journal*, Volume 52, pp. 1378-1391.

Vlachos, D. G., 2005. A review of multiscale analysis: Examples from systems biology, materials engineering, and other fluid-surface interacting systems. *Advances in Chemical Engineering*, Volume 30, pp. 1-61.